Synergy effects during current drive by two lower-hybrid waves

Youlei Yang, Nong Xiang, and Ye Min Hu

Citation: Physics of Plasmas **24**, 032502 (2017); doi: 10.1063/1.4977524
View online: http://dx.doi.org/10.1063/1.4977524
View Table of Contents: http://aip.scitation.org/toc/php/24/3
Published by the American Institute of Physics

PHYSICS OF PLASMAS **24**, 032502 (2017)

Synergy effects during current drive by two lower-hybrid waves

Youlei Yang,[1] Nong Xiang,[1,2,a)] and Ye Min Hu[1,2,b)]
[1]*Institute of Plasma Physics, Chinese Academy of Sciences, Hefei, Anhui 230031, People's Republic of China*
[2]*Center for Magnetic Fusion Theory, Chinese Academy of Sciences, Hefei, Anhui 230031, People's Republic of China*

(Received 13 January 2017; accepted 13 February 2017; published online 2 March 2017)

In recent lower-hybrid current drive experiments on the experimental advanced superconducting tokamak, two lower-hybrid waves are launched simultaneously from different locations with different phase velocities to drive the plasma current. To understand the synergy effects of the two LH waves, the analytical expression for the electron velocity distribution is obtained based on Fuchs' model [Fuchs *et al*., Phys. Fluids **28**(12), 3619–3628 (1985)], which is in good agreement with that obtained by solving the quasi-linear equation numerically via the CQL3D code [R. W. Harvey and M. G. McCoy, in *Proceedings of IAEA Technical Committee Meeting on Advances in Simulation and Modeling of Thermonuclear Plasmas, Montreal, Canada* (1992)]. The synergy factor is also obtained analytically. It is found that the existence of two resonant regions may bring more resonant electrons interacting with each wave and the perpendicular dynamics can further enhance the synergy effect by increasing the effective electron temperature, which in turn increases the number of electrons in the resonance with each wave. *Published by AIP Publishing.*
[http://dx.doi.org/10.1063/1.4977524]

I. INTRODUCTION

The steady state operation of tokamaks needs a non-inductive current drive to sustain and control the plasma current.[1] Lower-hybrid current drive (LHCD)[2–4] is the most effective radio-frequency (rf) current drive scheme at present, which has been applied in a wide range of present tokamaks,[5–7] and is planned to be used on ITER[8,9] and other future tokamak reactors such as CFETR.[10]

LHCD relies on the resonant interaction between plasmas and LH waves which causes the wave to transfer its momentum to the electrons, resulting in the formation of velocity-space plateau on the electron distribution function and the generation of current in the parallel direction. The steady-state electron distribution function comes from the balance of two effects in velocity-space. One is caused by the collisions, which tends to relax the electrons to a symmetric and isotropic Maxwellian distribution. The other is the quasilinear diffusion caused by the injected LH waves, which tends to drive the asymmetry of the distribution function that is necessary for the current drive.

In practical tokamak experiments, rf waves with different frequencies are often applied simultaneously for plasma heating and current drive. Experimental observations and kinetic calculations show that there are synergy effects among them.[11,12] The current driven by simultaneous usage of the waves might be significantly larger than the sum of the currents driven by the waves individually in the same plasma conditions. The high efficiency of LHCD and the high controllability of electron-cyclotron current drive (ECCD)[13,14] enable them to be a promising combination for maintaining and controlling of the plasma current. The synergy effects between LHCD and ECCD have been studied intensively.[15–18] It is found that the synergy effects come from the interaction of the velocity-space diffusions induced by the two waves: the EC wave pulling low-energy electrons out of the Maxwellian bulk and the LH wave driving them to high parallel velocities.

In recent LHCD experiments on the Experimental Advanced Superconducting Tokamak (EAST), two LH waves with the frequencies 2.45GHz and 4.6 GHz, respectively, are launched from each waveguide grill located at different windows.[19] The wave-induced diffusion in velocity space by one LH wave could affect the diffusion induced by the other one, and the interplay may yield strong synergy effects. Experimental investigations found that when two LH waves with different phase velocities are injected simultaneously into the plasma, the absorption of the LH wave with higher phase velocity can be enhanced.[20,21] Vlasov simulations suggest that the synergy effects between the fast and the slow spectrum of the LH waves could lead to a rapid spreading of the spectrum and a rapid formation of an elongated plateau of the distribution function.[22] While the interplay of the wave-induced diffusions in velocity-space still requires systematic investigations by simulation and analysis. Meanwhile, an accurate and efficient model is needed for quantitative studies of the steady-state distribution function and the synergy factor.

In this paper, synergy effects between two LH waves with different phase velocities are investigated by solving the Fokker-Planck equation with the diffusions induced by the two LH waves analytically and numerically. An analytical solution of the equation is derived based on Fuchs' model. The expressions for the steady-state electron distribution function and the synergy factor are obtained. The analytical model captures the key factors of the synergy effects and

a)Electronic mail: xiangn@ipp.ac.cn
b)Electronic mail: yeminhu@ipp.ac.cn

provides an efficient way to calculate the driven currents and the synergy factors. The numerical methods provide accurate solutions of the Fokker-Planck equations and methods to check the analytical model.

This article is organized as follows: The steady-state electron distribution function solutions for the collisional quasi-linear equation with diffusions induced by the two LH waves are presented in Sec. II, in which the synergy factor and the mechanism of the synergy effects are discussed. Conclusions and further discussions are given in Sec. III.

II. THEORETICAL MODEL FOR LHCD WITH TWO LOWER HYBRID WAVES

The evolution of the electron distribution function in the presence of collision and LH waves driving can be described by the quasi-linear equation with linearized collision operator at high-velocity limit[2]

$$\frac{\partial f}{\partial t} = \Gamma\left[\frac{1}{v^2}\frac{\partial}{\partial v}\left(\frac{v_T^2}{v}\frac{\partial f}{\partial v}+f\right)+\frac{1+Z_i-v_T^2/2v^2}{2v^3}\times\frac{\partial}{\partial\mu}\left(1-\mu^2\right)\frac{\partial}{\partial v}f\right]-\frac{\partial}{\partial v_\parallel}D_{LH}(v_\parallel)\frac{\partial}{\partial v_\parallel}f, \quad (1)$$

where f is the electron distribution function, $\mu \equiv v_\parallel/v$, $\Gamma \equiv nq^4\ln\Lambda/2\pi\varepsilon_0^2 m^2$, and $v_T = \sqrt{T_e/m_e}$ is the electron thermal velocity, D_{LH} is the quasilinear diffusion coefficient of LH waves. The first term on the right hand side of Eq. (1) describes the effects induced by collisions, which include the energy diffusion, the frictional deceleration, and the "pitch-angle" scattering.

When two LH waves with different phase velocities are launched into a plasma simultaneously, two velocity-space diffusions might be induced and interact with each other. To account for the interactions between electrons and the two LH waves, the quasilinear diffusion coefficient in Eq. (1) now contains the contributions of the two waves which is denoted as $D(w) = D_1(w) + D_2(w)$, where $D(w) = D_{LH}/\nu v_T^2$ is the normalized diffusion coefficient and $w = v_\parallel/v_T$ is the normalized parallel velocity. Here, $D_1(w)$ and $D_2(w)$ represent the quasi-linear diffusion coefficients induced by the LH waves at 2.45 GHz and 4.6 GHz, respectively. Note that the non-linear interactions of the electrons with the two LH waves[23] are not considered.

Different numerical codes have been developed to solve Eq. (1), such as LUKE[24] and CQL3D.[25] Although the numerical codes are very successful in calculating the electron distribution function, they are computationally expensive and lack the understanding of the physics. Here, we develop an analytical model to depict the synergetic features during LHCD with two LH waves.

To obtain an analytical solution of Eq. (1) with two velocity-space diffusions, we assume that both $w^3D_1(w) \gg 1$ and $w^3D_2(w) \gg 1$ in the resonance regions, as the rf diffusions dominate the collisional diffusion even with small rf power.[26] Therefore, the quasi-linear diffusions for the synergy case with two LH waves can be modeled as

$$D(w) = \begin{cases} D_0, & w \in [w_1, w_2] \cup [w_3, w_4] \\ 0, & \text{otherwise.} \end{cases} \quad (2)$$

Here, w_1, w_2, w_3, and w_4 are boundaries of the resonance regions and $D_0 \to \infty$. In general, the lower-hybrid waves are only resonant with fast electrons, i.e., $w_1 \gg 1$. So far, we take $w_1 \le w_2 \le w_3 \le w_4$, which means that the resonance regions do not overlap. Since $D(w) \to \infty$ in the resonance regions, the overlapped case with $w_1 \le w_3 \le w_2 \le w_4$ is identical to the case with resonance regions $w_1 \le w \le w_2$ and $w_2 \le w \le w_4$.

Following Fisch's assumption that the distribution function f in Eq. (1) is a Maxwellian in the perpendicular direction with a fixed temperature,[2] the steady-state parallel distribution function for the synergy case with two LH waves can be written as

$$F(w) = \begin{cases} C_{12}\exp\left(-\frac{w^2}{2}\right), & w < w_1, \\ C_{12}\exp\left(-\frac{w_1^2}{2}\right), & w_1 \le w \le w_2, \\ C_{12}\exp\left(\frac{w_2^2-w_1^2}{2}\right)\exp\left(-\frac{w^2}{2}\right), & w_2 \le w \le w_3, \\ C_{12}\exp\left(\frac{w_2^2-w_1^2}{2}\right)\exp\left(-\frac{w_3^2}{2}\right), & w_3 \le w \le w_4, \\ C_{12}\exp\left(\frac{w_2^2-w_1^2}{2}\right)\exp\left(\frac{w_4^2-w_3^2}{2}\right)\exp\left(-\frac{w^2}{2}\right), & w > w_4, \end{cases} \quad (3)$$

where C_{12} is a constant that could be determined by the normalization condition. The distribution function is local plateaus in the resonance regions and is local Maxwellian distributions outside. Then the current driven by the two waves simultaneously can be obtained by integrating Eq. (3) and can be written as

$$J_{12} = C_{12}\exp\left(-\frac{w_1^2}{2}\right)\frac{w_2^2 - w_1^2}{2} + C_{12}\exp\left(\frac{w_2^2 - w_1^2}{2}\right)\exp\left(-\frac{w_3^2}{2}\right)\frac{w_4^2 - w_3^2}{2}. \quad (4)$$

The currents driven by the two waves individually are

$$J_1 = C_1\exp\left(-\frac{w_1^2}{2}\right)\frac{\left(w_2^2 - w_1^2\right)}{2}, \quad (5)$$

$$J_2 = C_2\exp\left(-\frac{w_3^2}{2}\right)\frac{\left(w_4^2 - w_3^2\right)}{2}, \quad (6)$$

respectively. Note that the currents are normalized by $q_e n_e v_T$, where q_e is the elemental charge of the electron and n_e is the electron density. The normalization constants C_1, C_2, and C_{12} are mainly determined by the bulk electrons; the fast electrons caused by the rf diffusions have little effect on them. Thus, the constants could be taken to be equal for those three cases.

The synergy effect between the two LH waves on current driving could be quantified by the synergy factor defined as[12]

$$\eta = \frac{J_{12}}{J_1 + J_2}. \quad (7)$$

Thus, the synergy factor estimate based on Fisch's model could be obtained as

$$\eta \simeq 1 + \exp\left(\frac{w_2^2 - w_1^2}{2}\right)\frac{J_2}{J_1}, \quad (8)$$

$$= 1 + \exp\left(-\frac{w_3^2 - w_2^2}{2}\right)\frac{\left(w_4^2 - w_3^2\right)}{\left(w_2^2 - w_1^2\right)}. \quad (9)$$

Apparently, the synergy effect stems from the enhancement of the current driven by the wave with higher parallel phase velocity, and the existence of the slower LH wave brings more electrons to be resonant with the faster one. The enhancement factor $\exp\left[\left(w_2^2 - w_1^2\right)/2\right]$ is determined by the first resonance region only, while J_2 itself depends on the second resonance region. Both the enhancement factor and J_2 drop rapidly as the distance between the two resonance regions gets larger, so does the synergy effect.

Applying Fisch's 1D model to the synergy case with two LH waves is straightforward. The model keeps the key aspect of the synergy effect caused by the LH wave with a lower parallel phase velocity. However, the aspect of the synergy effect caused by the LH wave with a higher parallel phase velocity cannot be addressed in this model. It is also found that, in a single wave case, the height of the plateau in this model is a little lower than the 2D numerical results and the distribution function drops much faster at the higher velocity side of the resonance region.[27] The disagreement is caused by the neglect of perpendicular dynamics. As the rf waves lead to an increase in the perpendicular temperature, the assumption that the distribution is a Maxwellian with the bulk temperature in the perpendicular direction is no longer valid.

The neglect of perpendicular dynamics leads to the underestimate of the plateau height and the effective temperature in the high-velocity region. To include the perpendicular dynamics, Fisch and Karney obtained the asymptotic solution of Eq. (1) through matching the distribution function and its derivatives at the boundaries of the resonance region with the assumption $D_0 \gg 1$.[28] Fuchs presented a one-dimensional model with a proper account of the essential perpendicular dynamics by representing the distribution function as $f = f_M + \tilde{f}$, where f_M is the central thermal Maxwellian and $\tilde{f}$ is a perpendicularly broadened distribution of fast electrons.[29] In this work, we extend Fuchs' model to the two LH waves case, in which the parallel distribution function could be obtained as

$$F^s = \begin{cases} F^s_{p1}\exp\left(-\alpha^s_p\frac{w^2}{2}\right) + F_M(w) & w < w_1 \\ F^s_{p1} & w_1 \le w \le w_2 \\ \tilde{C}_1\exp\left(-\alpha^s_p\frac{w^2}{2}\right) + F_M(w) & w_2 \le w \le w_3 \\ F^s_{p2} & w_3 \le w \le w_4 \\ \tilde{C}_2\exp\left(-\alpha^s_p\frac{w^2}{2}\right) + F_M(w) & w > w_4, \end{cases} \quad (10)$$

where

$$F^s_{p1} = \frac{F_M(w_1)}{1 - \exp\left(-\alpha^s_p\frac{w_1^2}{2}\right)}, \quad (11)$$

$$\tilde{C}_1 = F^s_{p1}\exp\left(\alpha^s_p\frac{w_2^2 - w_1^2}{2}\right) - \exp\left(\alpha^s_p\frac{w_2^2}{2}\right)\left[F_M(w_2) - F_M(w_1)\right], \quad (12)$$

$$F^s_{p2} = \left[F^s_{p1} - F_M(w_2)\right]\exp\left(-\alpha^s_p\frac{w_3^2 - w_2^2}{2}\right) + F_M(w_3), \quad (13)$$

$$\tilde{C}_2 = \tilde{C}_1\exp\left(\alpha^s_p\frac{w_4^2 - w_3^2}{2}\right) - \exp\left(\alpha^s_p\frac{w_4^2}{2}\right)\left[F_M(w_4) - F_M(w_3)\right], \quad (14)$$

$$\alpha^s_p = \frac{2 + Z_i}{(1 + Z_i)T^s_p + 1}. \quad (15)$$

Here, T^s_p is the effective perpendicular temperature in the synergy case and could be determined by

$$2T^s_p \equiv \frac{\int_{w_1}^{w_2} v_\perp^2 F^s_{p1}\,dw_0 + \int_{w_3}^{w_4} v_\perp^2 F^s_{p2}\,dw_0}{\int_{w_1}^{w_2} F^s_{p1}\,dw_0 + \int_{w_3}^{w_4} F^s_{p2}\,dw_0}. \quad (16)$$

The results in Eq. (10) show that the parallel distribution function is constant in the resonance regions and is the linear combination of two Maxwellian distributions with different temperatures outside the resonance regions.

In order to validate the analytical model, we solve Eq. (1) using the analytical models and the CQL3D code with $D_0 = 1$, for typical parameters with $w_1 = 3$, $w_2 = 5$, $w_3 = 6$, and $w_4 = 8$. The normalized quasi-linear diffusion coefficient is presumably assumed to be infinite in the resonance regions. In fact, as will be shown later, the analytical solution is a good approximated solution as long as $Dw^3 \gg 1$. Fig. 1 shows the resulting parallel distribution function from the 2D numerical code, the one based on Fish's 1D theory in Eq. (3), the one from the extended Fuchs' model in Eq. (10), and the initial Maxwellian distribution. It is shown that the height of the first plateau predicted based on Fisch's model is a little lower than the numerical one. Meanwhile, the distribution function drops too fast at the higher velocity side of the first resonance region, which leads to the considerable underestimation of the plateau height at the second resonance region, while the height of the first plateau predicted by extended Fuchs' model agrees well with the numerical one. Moreover, the slope of the distribution functions at the higher side of the first resonance region is predicted accurately, too. Thus, the height of the second plateau could be predicted accurately. Those results indicate that the perpendicular dynamics is important and should be considered in the quantitative study of synergy effects.

The driven currents can be obtained by integrating the parallel distribution function in Eq. (10). In general cases with $w_2 - w_1 \geq 1$ and $w_4 - w_3 \geq 1$, the height of the second plateau in Eq. (13) is approximately

$$F^{s}_{p2} \simeq \exp\left(-\alpha^{s}_{p}\frac{w_3^2 - w_2^2}{2}\right)F^{s}_{p1}. \tag{17}$$

The driven currents based on Fuchs' model can be approximately written as

$$J_1 \simeq F_{p1}\frac{w_2^2 - w_1^2}{2}, \tag{18}$$

$$J_2 \simeq F_{p2}\frac{w_4^2 - w_3^2}{2}, \tag{19}$$

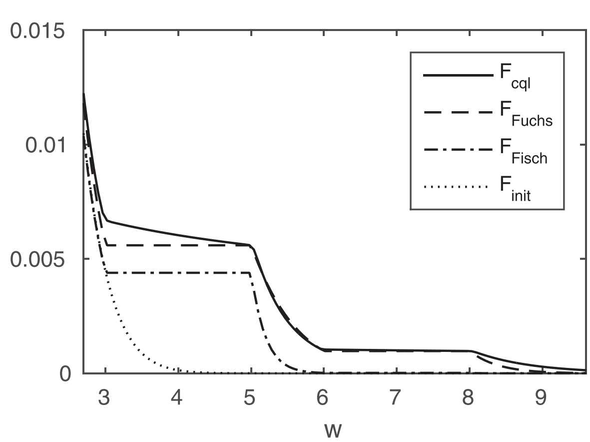

FIG. 1. Parallel distribution functions for a typical synergy case with $w_1 = 3$, $w_2 = 5$, $w_3 = 6$, $w_4 = 8$, and $D_0 = 1$. The solid line represents the numerical one from CQL3D, the dashed line represents the one form Fuchs' 1D model with perpendicular dynamics in Eq. (10), the dashed-dotted line represents the one from Fisch's 1D model in Eq. (3), and the dotted line represents the initial Maxwellian distribution.

$$J_{12} \simeq F^{s}_{p1}\frac{w_2^2 - w_1^2}{2} + F^{s}_{p2}\frac{w_4^2 - w_3^2}{2}, \tag{20}$$

where

$$F_{p1} = \frac{F_M(w_1)}{1 - \exp\left(-\alpha_{p1}\frac{w_1^2}{2}\right)}, \quad \text{with } \alpha_{p1} = \frac{2 + Z_i}{(1 + Z_i)T_{p1} + 1}, \tag{21}$$

$$F_{p2} = \frac{F_M(w_3)}{1 - \exp\left(-\alpha_{p2}\frac{w_3^2}{2}\right)}, \quad \text{with } \alpha_{p2} = \frac{2 + Z_i}{(1 + Z_i)T_{p2} + 1}, \tag{22}$$

with T_{p1} and T_{p2} estimated by

$$T_{p1} = \frac{1 + Z_i}{2 + Z_i}w_1(w_2 - w_1), \tag{23}$$

$$T_{p2} = \frac{1 + Z_i}{2 + Z_i}w_3(w_4 - w_3). \tag{24}$$

Then the synergy factor based on extended Fuchs' model could be obtained as

$$\eta \simeq g_s\left[1 + \exp\left(-\alpha^{s}_{p}\frac{w_3^2 - w_2^2}{2}\right)\frac{(w_4^2 - w_3^2)}{(w_2^2 - w_1^2)}\right], \tag{25}$$

where

$$g_s = \frac{1 - \exp(-\alpha_{p1}w_1^2/2)}{1 - \exp\left(-\alpha^{s}_{p}w_1^2/2\right)}. \tag{26}$$

The expression of the synergy factor in Eq. (25) reveals two aspects of the synergy effects. The first one can be seen in the expression of g_s. The factor $g_s = F^{s}_{p1}/F_{p1}$ is the ratio of the first plateau height with and without the LH wave with higher phase velocity, which represents the synergy effect caused by the faster LH wave. The injection of the LH wave with higher phase velocity further enhances the perpendicular temperature, i.e., $T^{s}_{p} > T_{p1}$, which leads to $\alpha^{s}_{p} < \alpha_{p1}$ then causes the plateau gets higher, i.e., $F^{s}_{p1} > F_{p1}$ according to Eqs. (11) and (21). This means more electrons are resonant with the LH wave with lower phase velocity, thus, driving more current. The other aspect of the synergy effects comes from the effect caused by the LH wave with lower phase velocity. This effect is also considered partially in Eq. (9), the difference is $\alpha^{s}_{p} < 1$ here, which stems from $T^{s}_{p} > 1$, i.e., the enhancement of the current driven by the faster LH wave is further enhanced due to the perpendicular effects. Note that if the perpendicular temperature is taken as the initial one, i.e., $T^{s}_{p} = T_{p1} = 1$, then Eqs. (25) and (9) are identical, which means that the synergy factor predicted based on Fisch's model is a special case of that predicted based on extended Fuchs' model.

To illustrate the interplay of the velocity-space diffusions induced by the two LH waves and the interaction between the electrons and the waves, the streamlines of the velocity-space flux and the non-Maxwellian part of the electron distribution function for the typical case are shown in Fig. 2. The LH wave with lower parallel phase velocity accelerates the electrons in the parallel direction and draws them out of the Maxwellian region in the velocity space. This will create local depressions, which tend to be smoothed by collisions. The electrons drawn into the resonant region are then further accelerated in the parallel direction by the quasi-linear rf diffusion and in the perpendicular direction by the pitch-angle scattering. A non-Maxwellian distribution function is created and spreads out of the resonant region by pitch-angle scattering, to the regions $w < w_1$ and $w > w_2$. The LH wave with higher parallel phase velocity acts like the slower wave when injected individually. When the two waves are injected simultaneously, the slower wave brings much more electrons, relative to the Maxwellian distribution, to the region $w_2 < w < w_3$. Thus, the faster wave could accelerate more electrons and drive more current. More electrons with relatively high energy will be produced, and the perpendicular temperature is increased further, which will also enhance the current drive of the slower wave. The current drive of the two waves is enhanced by each other, which results in the synergy effects.

The effect of $g_s > 1$ is relative to the height and width of the second plateau. Higher and wider plateau means more electrons with relative higher energy, which means higher perpendicular temperature. According to Eq. (17), the height of the second plateau strongly depends on the relative distance between the two resonance regions. As the distance between two resonance regions gets larger, the height of the second plateau drops sharply, and at the same time, the enhancement of the synergy effect gets smaller. This effect could be more clear by taking the width of the resonance regions to be identical, i.e., $w_2 - w_1 = w_4 - w_3 = W$, then using the integration in Eq. (16) and the definition of T_p for one LH wave case, the relations of the effective temperature can be represented as

$$T_p^s = T_{p1} + (1 - \alpha_T)(T_{p2} - T_{p1}), \tag{27}$$

with

$$\alpha_T = \frac{1}{1 + \exp\left(-\alpha_p^s \frac{w_3^2 - w_2^2}{2}\right)}. \tag{28}$$

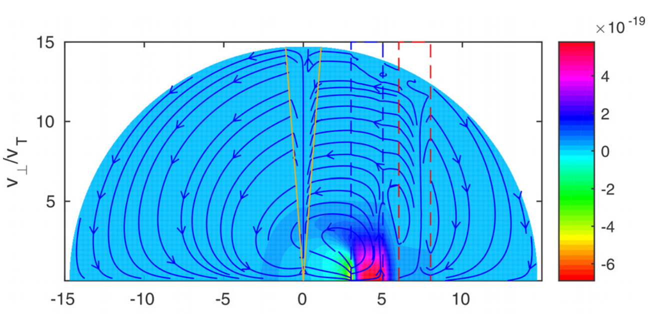

FIG. 2. Non-Maxwellian part of the distribution and streamlines of the velocity-space flux from CQL3D results, with $w_1 = 3$, $w_2 = 5$, $w_3 = 6$, $w_4 = 8$, and $D_0 = 1$.

As the value of $\exp[-\alpha_p^s(w_3^2 - w_2^2)/2]$ varies in (0, 1], the value of α_T varies in [0.5, 1); thus, $0 < (1 - \alpha_T) \leq 0.5$. The maximum value of $(1 - \alpha_T)$ is 0.5 when $w_3 - w_2 = 0$, i.e., the two resonance regions are conjoint. As the electrons in the second resonance region have relatively higher energy, we have $T_{p2} > T_{p1}$ in general cases. Thus, T_p^s has its maximum value of $(T_{p1} + T_{p2})/2$ when $w_3 - w_2 = 0$ and drops fast to T_{p1} as the distance between the two resonance regions $w_3 - w_2$ gets bigger.

According to Eqs. (18)–(20), the enhancement to the current driven by the LH wave with higher phase velocity strongly depends on the height and width of the first plateau, while the current driven by the second LH wave itself depends on the height and width of its own plateau. According to Eq. (17), this effect also drops sharply as the two resonance regions get farther away from each other.

By Eq. (25), the synergy effect is sensitive to the distance between the resonance regions and becomes weak rapidly as the distance increases. The synergy factors with $w_1 = 3$, $w_3 - w_2 \equiv \Delta$ varies from 0 to 2, and $w_2 - w_1 = w_4 - w_3 \equiv W$ varies from 0.5 to 4 are calculated using the numerical code CQL3D and the analytical model. The results are summarized in Fig. 3. It is shown that the synergy factors predicted by the analytical model agree well with the numerical ones. The synergy factor gets larger as the resonance region gets wider, while the synergy factor is more sensitive to the distance between the two resonance regions and decreases rapidly as the distance increases.

The synergy factors reach their maximum value when $\Delta = 0$, when the two resonance regions get closer and overlapped, i.e., $w_3 < w_2$, the resonance regions can be represented as $w_1 \leq w \leq w_2$ and $w_2 \leq w \leq w_4$, which means that the effective width of the second resonance region decreases by $w_2 - w_3$, and thus, the synergy factor will get smaller. Note that this is based on the assumption that $D(w)w^3 = D_0 \gg 1$ in the resonance regions, i.e., D_0 is large enough that its value has less effects on the results. To illustrate this effect, a series of cases with $w_1 = 3$, $w_2 = 5$, $w_4 - w_3 = 2$, and the

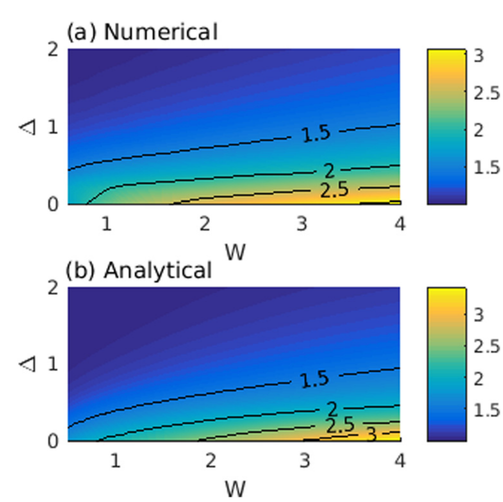

FIG. 3. Color and contour plot of the synergy factors with $w_1 = 3$, $w_3 - w_2 \equiv \Delta$ varies from 0 to 2, and $w_2 - w_1 = w_4 - w_3 \equiv W$ varies from 0.5 to 4 calculated by (a) the numerical code CQL3D and (b) the analytical model in Eq. (25).

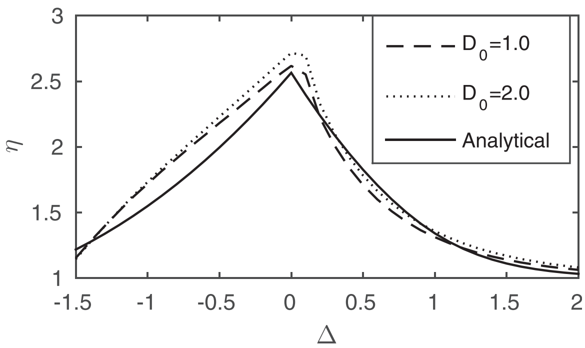

FIG. 4. The synergy factors with $w_1 = 3$, $w_2 = 5$, $w_4 - w_3 = 2$ and the distance between two resonance $w_3 - w_2 = \Delta$ varies from -1.5 to 2 are calculated by the analytical model and by the CQL3D code with $D_0 = 1$ and $D_0 = 2$.

distance between the two resonance regions $w_3 - w_2 \equiv \Delta$ varies from -1.5 to 2 are calculated by the analytical model and by the CQL3D code with $D_0 = 1$ and $D_0 = 2$. The resulting synergy factors as a function of the distance between the two resonance regions are shown in Fig. 4, which shows good agreement between the analytical results and the numerical ones, as long as $D_0 \geq 1$. It is also shown that the synergy factors calculated by CQL3D have negligible change as the diffusion coefficient is doubled, which means that $D_0 = 1$ is large enough for the solution to be insensitive to its precise magnitude.[27] For a typical plasma discharge on EAST with $n_e = 1 \times 10^{19} m^{-3}$, $T_e = 1\,keV$ and $B_\phi = 2T$, the LHW power needed to produce the normalized quasi-linear diffusion coefficient $D_0 = 1$ with $w_1 = 3$, $w_2 = 5$ is less than $100\,kW$, which is easy to reach during the LHCD experiments.

III. CONCLUSION AND DISCUSSION

In this work, the synergy effects of the two lower-hybrid waves are investigated by solving the Fokker-Planck equation analytically and numerically. The numerical results of CQL3D provide accurate solutions of the Fokker-Planck equation, but it is computationally expensive and lack the understanding of the physics.

Fisch's 1D theory is applied first to investigate the synergy effects. The results show that the synergy effects mainly arise from the enhancement of the current drive of the wave with the higher phase velocity. However, this model fails to calculate the enhancement quantitatively when the resonance regions of the two LH waves are separated. The distribution function drops too fast at the high-velocity side of the resonance region by the LH wave with the lower parallel phase velocity, which causes considerable underestimation of the current drive by the LH wave with the higher parallel phase velocity. It is found that the underestimation is caused by the invalid assumption that the perpendicular distribution function keeps a Maxwellian distribution with the bulk temperature. Meanwhile, the model cannot include the synergy effects caused by the LH wave with the higher parallel phase velocity.

The one-dimensional analytical model including the perpendicular dynamics of Fuchs' for single LH wave is extended to investigate the synergy effects during LHCD with two LH waves. The distribution functions, the driven currents, and the synergy factors predicted by this analytical model agree well with the numerical results as long as the input power is higher than 100 kW. The analytical model is also used to investigate the parameter dependencies of the synergy factors. It is found that the synergy factors are mostly sensitive to the relative distance between the two resonance regions. The synergy factor decreases rapidly when the distance increases, and reaches the maximum value when the two resonance regions are conjoint. This model is accurate and efficient for the investigation of synergy effects. It may be coupled to other models such as the transport codes and integrated modeling codes[30] for fast and accurate calculations of LHCD in tokamak plasmas.

So far, the investigations are taken in the velocity space, corresponding to a particular flux surface in a toroidal configuration. In the ray-tracing framework, the waves may pass through a certain flux surface several times. If the synergy effects are added to the ray-tracing process, the absorption of the waves will be affected, and then the synergy effects will change. This process should be repeated until a steady state is reached. Thus, an iterative progress must be applied to get the steady-state self-consistent results.[31] Note that there is a schema widely used for fast calculation of LHCD, in which the power absorption is calculated by solving the 1-D Fokker-Planck equation without considering the perpendicular heating by collisional pitch-angle scattering. The driven current is obtained by multiplying the power absorption with a current drive efficiency which is obtained from the models with only one resonance region in the velocity space. The analytical model presented in this paper could be used when the synergy effects affect the power absorption greatly.

The synergy effects enhance the absorption of the waves with higher phase velocity, which may be useful for the understanding of the spectra gap.[20] This effect may also cause the waves to be absorbed before propagating into the plasma core, and thus, tend to drive more off-axis current.[21]

ACKNOWLEDGMENTS

This work was supported by the National Natural Science Foundation of China under Grant Nos. 11475220, 11375234, 11575239, 11405218, and 11505227, the National ITER program of China under Contract No. 2013GB1120110, Program of Fusion Reactor Physics and Digital Tokamak with the CAS "One-Three-Five" Strategic Planning, the JSPS-NRF-NSFC A3 Foresight Program in the field of Plasma Physics (NSFC: No.11261140328 and NRF: No. 2012K2A2A6000443). Numerical computations were performed on the ShenMa High Performance Computing Cluster in Institute of Plasma Physics, Chinese Academy of Sciences.

[1]C. Gormezano, A. Sips, T. Luce, S. Ide, A. Becoulet, X. Litaudon, A. Isayama, J. Hobirk, M. Wade, T. Oikawa, R. Prater, A. Zvonkov, B. Lloyd, T. Suzuki, E. Barbato, P. Bonoli, C. Phillips, V. Vdovin, E. Joffrin, T. Casper, J. Ferron, D. Mazon, D. Moreau, R. Bundy, C. Kessel, A. Fukuyama, N. Hayashi, F. Imbeaux, M. Murakami, A. Polevoi, and H. S. John, Nucl. Fusion **47**, S285 (2007).

[2]N. J. Fisch, Phys. Rev. Lett. **41**, 873 (1978).
[3]P. T. Bonoli, E. Barbato, R. W. Harvey, and F. Imbeaux, AIP Conf. Proc. **694**, 24 (2003).
[4]Y. Peysson, J. Decker, E. Nilsson, J.-F. Artaud, A. Ekedahl, M. Goniche, J. Hillairet, B. Ding, M. Li, P. T. Bonoli, S. Shiraiwa, and M. Madi, Plasma Phys. Controlled Fusion **58**, 044008 (2016).
[5]J. Wilson, R. Parker, M. Bitter, P. Bonoli, C. Fiore, R. Harvey, K. Hill, A. Hubbard, J. Hughes, A. Ince-Cushman, C. Kessel, J. Ko, O. Meneghini, C. Phillips, M. Porkolab, J. Rice, A. Schmidt, S. Scott, S. Shiraiwa, E. Valeo, G. Wallace, J. Wright, and the Alcator C-Mod Team, Nucl. Fusion **49**, 115015 (2009).
[6]M. Goniche, V. Basiuk, J. Decker, P. Sharma, G. Antar, G. Berger-By, F. Clairet, L. Delpech, A. Ekedahl, J. Gunn, J. Hillairet, X. Litaudon, D. Mazon, E. Nilsson, T. Oosako, Y. Peysson, M. Preynas, M. Prou, and J. Ségui, Nucl. Fusion **53**, 033010 (2013).
[7]R. Cesario, L. Amicucci, C. Castaldo, M. Kempenaars, S. Jachmich, J. Mailloux, O. Tudisco, A. Galli, A. Krivska, and J.-E. contributors, Plasma Phys. Controlled Fusion **53**, 085011 (2011).
[8]G. Hoang, A. Bécoulet, J. Jacquinot, J. Artaud, Y. Bae, B. Beaumont, J. Belo, G. Berger-By, J. P. Bizarro, P. Bonoli, M. Cho, J. Decker, L. Delpech, A. Ekedahl, J. Garcia, G. Giruzzi, M. Goniche, C. Gormezano, D. Guilhem, J. Hillairet, F. Imbeaux, F. Kazarian, C. Kessel, S. Kim, J. Kwak, J. Jeong, J. Lister, X. Litaudon, R. Magne, S. Milora, F. Mirizzi, W. Namkung, J. Noterdaeme, S. Park, R. Parker, Y. Peysson, D. Rasmussen, P. Sharma, M. Schneider, E. Synakowski, A. Tanga, A. Tuccillo, and Y. Wan, Nucl. Fusion **49**, 075001 (2009).
[9]J. Decker, Y. Peysson, J. Hillairet, J.-F. Artaud, V. Basiuk, A. Becoulet, A. Ekedahl, M. Goniche, G. Hoang, F. Imbeaux, A. Ram, and M. Schneider, Nucl. Fusion **51**, 073025 (2011).
[10]Y. T. Song, S. T. Wu, J. G. Li, B. N. Wan, Y. X. Wan, P. Fu, M. Y. Ye, J. X. Zheng, K. Lu, X. Gao *et al.*, IEEE Trans. Plasma Sci. **42**, 503 (2014).
[11]B. Wan and J. Li for HT-7 Team, Nucl. Fusion **43**, 1279 (2003).
[12]S. Y. Chen, B. B. Hong, Y. Liu, W. Lu, J. Huang, C. J. Tang, X. T. Ding, X. J. Zhang, and Y. J. Hu, Plasma Phys. Controlled Fusion **54**, 115002 (2012).
[13]N. J. Fisch and A. H. Boozer, Phys. Rev. Lett. **45**, 720 (1980).
[14]R. Prater, Phys. Plasmas **11**, 2349 (2004).
[15]G. Giruzzi, J. F. Artaud, R. J. Dumont, F. Imbeaux, P. Bibet, G. Berger-By, F. Bouquey, J. Clary, C. Darbos, A. Ekedahl, G. T. Hoang, M. Lennholm, P. Maget, R. Magne, J. L. Ségui, A. Bruschi, and G. Granucci, Phys. Rev. Lett. **93**, 255002 (2004).
[16]W. Wei, B.-J. Ding, Y. Peysson, J. Decker, M.-H. Li, X.-J. Zhang, X.-J. Wang, and L. Zhang, Chin. Phys. B **25**, 015201 (2016).
[17]V. Ridolfini, E. Barbato, A. Bruschi, R. Dumont, F. Gandini, G. Giruzzi, C. Gormezano, G. Granucci, L. Panaccione, Y. Peysson, S. Podda, A. Saveliev, F. Team, and E. Team, "Radio frequency power in plasmas," in *14th Topical Conference on Radio Frequency Power in Plasmas, OXNARD, CA, 07–09 May, 2001* [AIP Conf. Proc. **595**, 225 (2001)].
[18]R. J. Dumont and G. Giruzzi, Phys. Plasmas **11**, 3449 (2004).
[19]M. H. Li, B. J. Ding, F. K. Liu, J. F. Shan, M. Wang, H. D. Xu, L. Liu, H. C. Hu, X. J. Zhang, Y. C. Li, W. Wei, Z. G. Wu, W. D. Ma, Y. Yang, J. Q. Feng, H. Jia, X. J. Wang, D. J. Wu, M. Chen, L. Xu, J. Wang, S. Y. Lin, J. Z. Zhang, J. P. Qian, Z. P. Luo, Q. Zang, X. F. Han, H. L. Zhao, Y. Peysson, J. Decker, A. Ekedahl, J. Hillairet, M. Goniche, and E. Team, Phys. Plasmas **23**, 102512 (2016).
[20]S. Ide, O. Naito, T. Kondoh, Y. Ikeda, and K. Ushigusa, Phys. Rev. Lett. **73**, 2312 (1994).
[21]W. Mao, D. Bojiang, X. Handong, Z. Lianmin, L. Liang, L. Shiyao, X. Ping, S. Youwen, H. Huaichuan, Y. Yong, J. Hua, W. Xiaojie, W. Dongxia, Q. Yongliang, F. Jianqiang, L. Fukun, S. Jiafang, and Z. Yanping, Plasma Sci. Technol. **11**, 534 (2009).
[22]S. J. Karttunen, T. J. H. Pättikangas, R. R. E. Salomaa, M. Shoucri, I. Shkarofsky, P. Bertrand, and A. Ghizzo, Phys. Scr. **60**, 356 (1999).
[23]Y. Huang, N. Xiang, G. Jia, D. Li, X. Wang, and Y. Lin, Phys. Plasmas **23**, 092114 (2016).
[24]J. Decker and Y. Peysson, Report No. EUR-CEA-FC-1736 Euratom-CEA (2004).
[25]R. W. Harvey and M. G. McCoy, in *Proceedings of IAEA Technical Committee Meeting on Advances in Simulation and Modeling of Thermonuclear Plasmas, Montreal, Canada* (1992), p. 489.
[26]N. J. Fisch, Rev. Mod. Phys. **59**, 175 (1987).
[27]C. F. F. Karney and N. J. Fisch, Phys. Fluids **22**, 1817 (1979).
[28]N. J. Fisch and C. F. F. Karney, Phys. Fluids **28**, 3107 (1985).
[29]V. Fuchs, R. A. Cairns, M. M. Shoucri, K. Hizanidis, and A. Bers, Phys. Fluids **28**, 3619 (1985).
[30]G. Falchetto, D. Coster, R. Coelho, B. Scott, L. Figini, D. Kalupin, E. Nardon, S. Nowak, L. Alves, J. Artaud, V. Basiuk, J. P. Bizarro, C. Boulbe, A. Dinklage, D. Farina, B. Faugeras, J. Ferreira, A. Figueiredo, P. Huynh, F. Imbeaux, I. Ivanova-Stanik, T. Jonsson, H.-J. Klingshirn, C. Konz, A. Kus, N. Marushchenko, G. Pereverzev, M. Owsiak, E. Poli, Y. Peysson, R. Reimer, J. Signoret, O. Sauter, R. Stankiewicz, P. Strand, I. Voitsekhovitch, E. Westerhof, T. Zok, W. Zwingmann, I.-T. Contributors, the ASDEX Upgrade Team, and J.-E. Contributors, Nucl. Fusion **54**, 043018 (2014).
[31]P. T. Bonoli and R. C. Englade, Phys. Fluids **29**, 2937 (1986).